

Effects of Neutral Hydrogen on Cosmic Ray Precursors in Supernova Remnant Shock Waves

John C. Raymond,¹ J. Vink,² E.A. Helder,² & A. de Laat²

ABSTRACT

Many fast supernova remnant shocks show spectra dominated by Balmer lines. The $H\alpha$ profiles have a narrow component explained by direct excitations and a thermally Doppler broadened component due to atoms that undergo charge exchange in the post-shock region. However, the standard model does not take into account the cosmic-ray shock precursor, which compresses and accelerates plasma ahead of the shock. In strong precursors with sufficiently high densities, the processes of charge exchange, excitation and ionization will affect the widths of both narrow and broad line components. Moreover, the difference in velocity between the neutrals and the precursor plasma gives rise to frictional heating due to charge exchange and ionization in the precursor. In extreme cases, all neutrals can be ionized by the precursor.

In this paper we compute the ion and electron heating for a wide range of shock parameters, along with the velocity distribution of the neutrals that reach the shock. Our calculations predict very large narrow component widths for some shocks with efficient acceleration, along with changes in the broad- to-narrow intensity ratio used as a diagnostic for the electron-ion temperature ratio. Balmer lines may therefore provide a unique diagnostic of precursor properties. We show that heating by neutrals in the precursor can account for the observed $H\alpha$ narrow component widths, and that the acceleration efficiency is modest in most Balmer line shocks observed thus far.

Subject headings: shock waves — acceleration of particles — ISM: supernova remnants

1. Introduction

Cosmic rays are widely believed to originate in supernova remnant (SNR) shock waves, because the cosmic-ray energy spectrum agrees with model predictions, because power-law distributions of energetic electrons are seen in SNRs, and because the power required to maintain the cosmic ray population could be supplied by about 10% of kinetic energy of Galactic supernovae. The standard theory for the process is Diffusive Shock Acceleration (DSA), which is a first order Fermi process requiring that particles scatter between a gasdynamic subshock and plasma turbulence in a shock pre-

cursor. Evidence for non-linear DSA comes from curved synchrotron spectra (Reynolds & Ellison 1992; Vink et al. 2006; Allen et al. 2008), evidence for high compression factors (Warren et al. 2005; Cassam-Chenaï et al. 2008) and evidence for lower than expected downstream temperatures (Hughes et al. 2000; Helder et al. 2009). However, all this evidence is based on observation of downstream properties. The effects of precursor physics on the $H\alpha$ emission described here offer a direct probe of the properties of the precursor.

A crucial parameter for these models is the diffusion coefficient κ , as it determines the precursor scale length, which is typically κ divided by the shock speed V_S . Gas is compressed in the precursor and accelerated to a fraction of the shock speed, and this compression is related to V_S , to the efficiency of particle acceleration and to the escape of energetic particles from the region (Bykov

¹Harvard-Smithsonian Center for Astrophysics, 60 Garden St., Cambridge, MA 02138, USA; jraymond@cfa.harvard.edu

²Astronomical Institute, Utrecht University, P.O. Box 80000, 3508TA Utrecht, The Netherlands

2005; Vink et al. 2010). Neutrals can impede the acceleration process by damping the turbulence needed to scatter particles back to the shock. However, Drury et al. (1996) found that the acceleration efficiency can be high as long as the density and neutral fraction are not too large, though the maximum particle energy is reduced.

One set of diagnostics for the physics of collisionless shocks is based on the emission from particles in the narrow ionization zone just behind a nonradiative shock (Raymond 1991; Heng 2010). In particular, $H\alpha$ photons from a non-radiative shock in partly neutral gas originate very close to the shock, and Coulomb collisions do not have time to erase such signatures as unequal electron and ion temperatures or non-Maxwellian velocity distributions (Laming et al. 1996; Ghavamian et al. 2001; Raymond et al. 2008, 2010). In the optical these shocks are seen as pure Balmer line filaments whose profiles show a narrow component characteristic of the pre-shock kinetic temperature and a broad component closely related to the post-shock proton temperature (Chevalier & Raymond 1978; Heng 2010; van Adelsberg et al. 2008). The intensity ratio of the broad and narrow components is determined by the electron to ion temperature ratio at the shock (Ghavamian et al. 2001; van Adelsberg et al. 2008; Helder et al. 2010).

The Balmer line profiles also contain signatures of shock precursors. In general, the narrow component line widths are 40 to 50 km s^{-1} , indicating temperatures around 40,000 K. If that were the ambient ISM temperature, there would be no neutrals to create the Balmer line filament, so the width is interpreted as an indication of heating in a narrow precursor too thin to completely ionize the hydrogen (Smith et al. 1994; Hester et al. 1994; Lee et al. 2007; Sollerman et al. 2003). Faint emission ahead of the sharp filament is interpreted as emission from the compressed and heated precursor gas (Hester et al. 1994; Lee et al. 2007, 2010).

This paper considers the role of neutrals in heating the precursor plasma and computes the properties of precursor $H\alpha$ emission. While cosmic ray pressure in the precursor can compress, heat and accelerate ions and electrons by means of plasma turbulence and magnetic fields, the neutrals only interact with the precursor by means of

collisions with protons and electrons. If the density is very high, neutrals and protons are tightly coupled by charge transfer. In that case, the neutrals are compressed along with the protons and adiabatically heated. They also share in any other heating of the protons, such as dissipation of Alfvén waves generated by cosmic-ray streaming. On the other hand, if the density is very low, neutrals pass through the precursor and the shock without interacting at all, preserving their pre-shock velocity distribution.

The intermediate case is more complex. A shock that efficiently accelerates cosmic rays is strongly modified, and gas reaches a significant fraction of the shock speed in the precursor (Vladimirov et al. 2008; Wagner et al. 2009). If neutrals and ions are fairly well coupled, they can be described as fluids whose relative speed gives a frictional heating similar to that in C-shocks (Draine & McKee 1993). If a neutral encounters this high speed compressed plasma without having been brought gradually up to speed by many previous charge transfers, it can be ionized and become a pickup ion (Raymond et al. 2008; Ohira & Takahara 2010) like those observed in the solar wind (Moebius et al. 1985). It can then have an energy on the order of 1 keV, which it can share with the other protons. Electron heating is more uncertain, but it can occur by means of Lower Hybrid waves (Cairns & Zank 2002). If the electrons are heated they can excite and ionize H atoms, changing the $H\alpha$ profile and the broad-to-narrow line ratio used as an electron temperature diagnostic (Ghavamian et al. 2001).

In this paper we compute the proton, neutral and electron temperatures in the precursors for a variety of parameters, along with the ionization and excitation of H atoms. We consider the effects of these processes on Balmer line diagnostics currently in use. Ohira & Takahara (2010) considered the effects of neutrals on the velocity structure of the precursor, the compression ratio and the acceleration process. They found that the pickup ions can reduce the compression by the subshock and enhance proton injection into the acceleration process. Morlino et al. (2010) self-consistently computed the particle acceleration and heating due to neutrals, but within the fluid approximation for both neutrals and ions. In this paper we emphasize the effects on the $H\alpha$ line

profile.

2. Model Calculations

We parameterize the precursor structure in a relatively simple manner. We assume that the precursor accelerates and compresses the interstellar gas over a length scale κ/V_S , where κ is the diffusion coefficient for cosmic rays near the cutoff. Effective cosmic-ray acceleration requires κ on the order of $10^{24} \text{ cm}^2 \text{ s}^{-1}$, and estimates based on the scales of H α precursors are 2 to $4 \times 10^{24} \text{ cm}^2 \text{ s}^{-1}$ (Lee et al. 2007, 2010). We do not consider the second order effects of momentum and energy deposition by the neutrals on the precursor length scale.

We assume an exponential form, so that the compression is given by

$$\chi = 1 + (\chi_1 - 1) e^{(xV_S/\kappa)} \quad (1)$$

where x is negative ahead of the shock and χ_1 is the compression ratio just upstream of the subshock. It is related to the fractional pressure of cosmic rays behind the shock, $w = P_{CR}/(P_G + P_{CR})$, by equation 9 of Vink et al. (2010). We simplify this equation with the assumption that for $w < 0.8$ the compression in the gas subshock equals 4, so that

$$\chi_1 = (1 - w/4)/(1 - w) \quad (2)$$

Mass conservation implies velocities $V = V_S/\chi$ in the frame of the shock.

To compute the proton and electron temperatures we include adiabatic compression, Coulomb energy transfer between protons and electrons, energy losses due to ionization and excitation of Hydrogen, and heating terms.

We assume that any neutral that interacts with the plasma at position x_i joins the proton flow at that position. If the interaction was charge transfer, a new neutral is formed with the bulk speed and thermal speed of the protons at x_i . Thus the neutrals arriving at x_i are those that last went through charge transfer at all upstream positions x_j , and they have the speeds, v_j , of the plasma at x_j . Each ionization of a neutral from x_j at x_i deposits energy $0.5m_p(v_j - v_i)^2$. We assume that the energy is quickly thermalized among the protons, unlike Ohira & Takahara (2010), who as-

sumed a pickup ion velocity distribution. The thermalization time scale is very uncertain, because full kinetic calculations have not been carried out. However, in the highly turbulent precursor there are many wave modes besides Alfvén waves that can thermalize the protons, in particular those associated with bump-on-tail, mirror and firehose-like instabilities (Winske et al. 1985; Gary 1978; Sagdeev et al. 1986). We also ignore heating due to Alfvén wave damping or shocks excited by the cosmic-ray pressure gradient in order to isolate the effect of the neutrals. Therefore, we compute a lower limit to the heating.

For electrons, we follow Cairns & Zank (2002), who found that ionization of fast neutrals forms a ring beam, in which all the particles gyrate around the magnetic field with the same speed but different phases. The ring beam is unstable, and provided that the beam velocity (in this case the relative velocity of bins i and j) is less than 5 times the Alfvén speed, it transfers a significant amount of heat to electrons via Lower Hybrid waves. We follow Cairns & Zank (2002) in taking this fraction to be 10%. Again, to isolate the effects of neutrals we ignore any heating of electrons by Lower Hybrid waves generated by cosmic-ray streaming (Ghavamian et al. 2007; Rakowski et al. 2008).

Charge transfer rates are taken from (Schultz et al. 2008) using the quadrature sum of the thermal speed and the ion-neutral relative speed. Ionization and excitation rates are computed from cross sections from Janev & Smith (1993) by integrating over the electron velocity distribution including the relative electron-neutral flow speed.

3. Results

Figure 1 shows a set of models for a shock speed of 2000 km s^{-1} with $\kappa = 2.0 \times 10^{24} \text{ cm}^2 \text{ s}^{-1}$, a pre-shock density of 0.2 cm^{-3} and a neutral fraction of 0.2. The four models have ratios of cosmic-ray partial pressure to total pressure behind the subshock, w , of 0.1, 0.3, 0.5 and 0.7. The compression ratios just ahead of the subshock are 1.0833, 1.3214, 1.75 and 2.75. In the high V_S , high efficiency models the neutrals are not compressed to this level, because of collisional ionization and because some pass through without charge transfer. The protons and electrons are strongly heated in the more efficient models, but the electrons are

much cooler than the protons. The drop in heating just before the subshock in the 70% efficient model results from the reduced number of neutrals.

Figure 2 shows the velocity distributions of the neutrals perpendicular to the shock just before the subshock. Note that the w=50% model shows a narrow component due to neutrals that last experience charge transfer far upstream, along with a broader component of particles that undergo charge transfer close to the subshock.

Figure 3 shows a grid of models of the neutral velocity distribution at the shock for a range of shock speeds and cosmic-ray partial pressures. The panels show the FWHM measured directly from the computed velocity distribution and the kurtosis, which would be 3.0 for a Gaussian distribution. Kurtosis is a problematic statistical moment for real data because it is sensitive to noise far from the line center and the choice of background level. However, for the theoretical profiles computed here it highlights cases in which some neutrals undergo charge transfer close to the subshock and others do not. We also show the fraction of incident neutrals that survive up to the subshock and the average number of excitations to the n=3 level per incident H atom. Not all of these excitations will result in H α photons because some Ly β photons escape, but this is a convenient comparison to the 0.2 to 0.25 H α photons per H atom produced in the post-shock region.

4. Discussion

The interaction of neutral hydrogen with the ionized plasma in cosmic-ray precursors described above offers an important tool to measure the properties of cosmic-ray precursors. The outcome of DSA is very much influenced by physical processes in the precursor, which are not well determined. For example, non-adiabatic heating and magnetic field amplification due to the presence of cosmic rays tend to decrease the overall compression factor from $\chi_{12} \gg 20$ (e.g. Berezhko & Ellison 1999; Blasi et al. 2005) to $7 \lesssim \chi_{12} \lesssim 15$ (Vladimirov et al. 2008; Caprioli et al. 2008). In addition, if the Alfvén waves in the precursor have some drift velocity this will affect the cosmic-ray pressure profile (Zirakashvili & Ptuskin 2008), which limits the escape of energy from the shock region. A lower

energy escape automatically implies a lower downstream cosmic-ray pressure (Vink et al. 2010).

As shown here, neutrals will influence the physics of the precursor. Morlino et al. (2010) treated the neutrals as a fluid coupled to the ions by charge transfer for a unified treatment of the heating and dynamics of the precursor, but the fluid approximation is only appropriate if neutrals and ions are coupled fairly well. They obtained a FWHM of 46 km s⁻¹ for the H α line in a 2000 km s⁻¹ shock with modest efficiency, a pre-shock density of 1 cm⁻³ and 50% neutral fraction. For similar parameters we find a non-Maxwellian profile with smaller FWHM and broader wings.

Neutrals can also damp plasma waves, which limits the efficiency of cosmic-ray acceleration. This damping is caused by the central processes described above: charge exchange and ionization. Drury et al. (1996) found that the maximum particle energy, and therefore the maximum acceleration efficiency, is considerably higher than suggested by Draine & McKee (1993). In addition, the heating due to neutrals penetrating the precursor is a form of non-adiabatic heating. Energy dissipated in the precursor limits the amount of free energy available for shock acceleration. If the neutrals ionized in the precursor behave as pickup ions rather than thermalizing with the protons, the injection efficiency and particle spectrum will be affected (Ohira & Takahara 2010). In any case, the heating of electrons in the precursor is poorly known, and that will strongly affect the ionization and excitation of H atoms, which in turn will affect the intensity ratio of the broad and narrow components as well as the narrow component line width.

The physics of neutral-ion coupling means these processes are not only sensitive to cosmic-ray pressure and the structure of the precursor, but also to the pre-shock density and neutral fraction. For example, the protons and neutrals in the Cygnus Loop nonradiative shocks (Salvesen et al. 2009) are tightly coupled, and they behave nearly adiabatically, while the pre-shock density in SN1006 is so low (Acero et al. 2007) that neutrals pass straight through it. This may explain the narrow line width seen by Sollerman et al. (2003) in SN 1006 in comparison to broader narrow lines observed for other young SNRs. The number of charge transfer events for an average neutral in

the precursor can be estimated roughly as

$$N_{CT} = nL\sigma\chi_1/V_S, \quad (3)$$

where L is the precursor length scale, and the charge transfer cross section, σ , declines slowly with velocity below about 2000 km s^{-1} , then very rapidly.

Comparing our results to observations, it is obvious that the observed narrow-line $H\alpha$ widths are in general smaller than predicted by our calculations for efficient shock acceleration (i.e., $w > 0.5$). This may indicate that none of the shocks investigated so far accelerate particles efficiently. However, more work is needed before such a conclusion can be drawn, as the line width depends also on pre-shock density and shock velocity. For very high shock velocities combined with low densities the neutrals hardly interact in the precursor, leading to narrow line widths. Such may be the case for the northeastern region of RCW 86, for which Helder et al. (2009) reported a high cosmic-ray acceleration efficiency ($w \gtrsim 0.5$, see also Vink et al. 2010). For this region the pre-shock density may be as low as $n \lesssim 0.1$ (Vink et al. 2006), which, combined with the high velocity ($V_s \gtrsim 3000 \text{ km/s}$), gives few interactions in the precursor and widths $\lesssim 100 \text{ km/s}$. Note that this is smaller than could be measured given the moderate spectral resolution of the measurement.

Perhaps the most striking result from these calculations is that for efficient shocks near 1000 km s^{-1} a substantial number of $H\alpha$ photons will be produced in the precursor. These will usually be included in the narrow component, potentially affecting the electron temperature estimate based on the broad-to-narrow intensity ratio (Ghavamian et al. 2001). Narrow component emission from the precursor could explain the broad-to-narrow intensity ratios that cannot be fit by models of post-shock emission (van Adelsberg et al. 2008; Rakowski et al. 2009). In extreme cases, emission from the precursor might also contribute to the broad component, possibly accounting for the non-Maxwellian profile seen in Tycho's SNR (Raymond et al. 2010) and generally leading to an underestimate of the shock speed. Both of these conclusions depend on the diffusion coefficient and the electron heating,

however.

Other $H\alpha$ line measurements show that the narrow lines are broader than one might expect for temperatures of typical HII regions, but smaller than 50 km/s (Sollerman et al. 2003). (Not all of the narrow line emission comes from the precursor, but the narrow line emission downstream is determined by the velocity distribution in the precursor.) Another effect of charge exchange in the precursor is that neutrals enter the downstream shock region with a velocity offset with respect to the local interstellar medium, as seen in Tycho's supernova remnant (Lee et al., 2007). For shocks observed face on this should produce a narrow line offset, which for the combined front and back side of the remnant should lead to two narrow lines. The spectra of several LMC remnants (Smith et al. 1994) do not show such an effect. For one of the remnants in this set, SNR 0509-67.5, the cosmic-ray acceleration efficiency was estimated to be $w \approx 0.2$ (Helder et al. 2010).

We note that several improvements should be made to the calculations presented here. Additional heating due to wave dissipation can heat the protons, resulting in larger narrow component line widths, or it can heat electrons, increasing the $H\alpha$ narrow component intensity and reducing the number of neutrals that reach the shock, especially if the electron velocity distribution is non-Maxwellian (Laming & Lepri 2007). In addition, ionization and excitation by proton and helium ion impact are important at high relative velocities (Laming et al. 1996), and at high shock speeds the velocity distributions of particles are anisotropic (Heng & McCray 2007; Heng et al. 2007; van Adelsberg et al. 2008). Amplification of the magnetic field may also be important, and radiative transfer calculations in the $Ly\beta$ line must be done to compute the $H\alpha$ emission. We plan to address these issues in future work.

This work was carried out while JCR was visiting the Astronomical Institute Utrecht as Minnaert Professor. It was supported by NASA grant GO-11184.01-A-R to the Smithsonian Astrophysical Observatory. JV and EH are supported by the VIDI grant awarded to JV by the Netherlands Science Foundation (NWO).

REFERENCES

- Acero, F., Ballet, J. & Decourchelle, A. 2007, *A&A*, 475, 883
- Allen, G.E., Houck, J.C. & Sturmer, S.J. 2008, *ApJ*, 683, 773
- Berezhko, E.G. & Ellison, D.G. 1999, *ApJ*, 526, 385
- Blasi, P., Gabici, S., & Vannoni, G. 2005, *MNRAS*, 361, 907
- Bykov, A. 2005, *Ad. Sp. Res.*, 36, 738
- Cairns, I.H. & Zank, G.P. 2002, *Geophys. Res. Lett.*, 29, 47
- Caprioli, D., Blasi, P., Amato, E. & Vietri, M. 2008, *ApJ*, 679, L139
- Cassam-Chenaï, G., Hughes, J.P., Reynoso, E.M., Badenes, C. & Moffett, D. 2008, *ApJ*, 680, 1180
- Chevalier, R.A., & Raymond, J.C. 1978, *ApJL*, 225, L27
- Draine, B.T. & McKee, C.F. 1993, *ARA&A*, 31, 373
- Drury, L.O., Duff, P., & Kirk, J.G. 1996, *A&A*, 309, 1002
- Gary, S.P. 1978, *JGR*, 85, 2304
- Ghavamian, P., Raymond, J.C., Smith, R.C., & Hartigan, P. 2001, *ApJ*, 547, 995
- Ghavamian, P., Laming, J.M. & Rakowski, C.E. 2007, *ApJ*, 645, L69
- Helder, E.A., Vink, J., Bassa, C.G., Bamba, A., Bleeker, J.A.M., Funk, S., Ghavamian, P., van der Heyden, K.J., Verbunt, F. & Yamazaki, R. 2009, *Science*, 325, 719
- Helder, E.A., Kosenko, D. & Vink, J. 2010, *ApJ*, 719, L14
- Helder, E.A. 2010, PhD thesis, Utrecht University
- Heng, K. 2010, *PASA*, 27, 23
- Heng, K., & McCray, R. 2007, *ApJ*, 654, 923
- Heng, K., van Adelsberg, M., McCray, R., & Raymond, J.C. 2007, *ApJ*, 668, 275
- Hester, J.J., Raymond, J.C., & Blair, W.P. 1994, *ApJ*, 420, 721
- Hughes, J.P., Rakowski, C.E., Decourchelle, A. 2000, *ApJ*, 543, L61
- Janev, R.K. & Smith, J.J. 1993, Cross Sections for Collisional Processes of Hydrogen Atoms with Electrons, Protons and Multiply Charged Ions (Vienna: Int. At. Energy Agency)
- Laming, J.M., Raymond, J.C., McLaughlin, B.M. & Blair, W.P. 1996, *ApJ*, 472, 267
- Laming, J.M. & Lepri, S.T. 2007, *ApJ*, 660, 1642
- Lee, J.-J., Koo, B.-C., Raymond, J.C., Ghavamian, P., Pyo, T.-S., Tajitsu, A., & Hayashi, M. 2007, *ApJ*, 659, L133
- Lee, J.-J., Raymond, J.C., Park, S., Blair, W.P., Ghavamian, P., Winkler, P.-F. & Korreck, K. 2010, *ApJ*, 715, L146
- Moebius, E., Hovestadt, D., Klecker, B., Scholer, M., & Gloeckler, G. 1985, *Nature*, 318, 426
- Morlino, G., Amato, E., Blasi, P. & Caprioli, D. 2010, *astro-ph* 1012:2966
- Ohira, Y. & Takahara, F. 2010, *ApJ*, 721, L43
- Rakowski, C.E., Laming, J.M., & Ghavamian, P. 2008, *ApJ*, 684, 408
- Rakowski, C.E., Ghavamian, P. & Laming, J.M. 2009, *ApJ*, 696, 2195
- Raymond, J.C. 1991, *PASP*, 103, 781
- Raymond, J.C., Isenberg, P.A., & Laming, J.M. 2008, *ApJ*, 682, 408
- Raymond, J.C., Winkler, P.F., Blair, W.P., Lee, J.-J. & Park, S. 2010, *ApJ*, 712, 901
- Reynolds S.P. & Ellison, D.G. 1992, *ApJ*, 399, L75
- Sagdeev, R.Z., Shapiro, V.D., Shevchenko, V.I. & Szego, K. 1986, *GRL*, 13, 85
- Salvesen, G.R., Raymond, J.C., & Edgar, R.J. 2009, *ApJ*, 702, 327
- Schultz, D.R., Krstic, P.S., Lee, T.G. & Raymond, J.C. 2008, *ApJ*, 678, 950

- Smith, R.C., Kirshner, R.P., Blair, W.P., & Winkler, P.F. 1991, ApJ, 375, 652
- Sollerman, J., Ghavamian, P., Lundqvist, P. & Smith, R.C. 2003, A&A, 407, 249
- van Adelsberg, M., Heng, K., McCray, R., & Raymond, J.C. 2008, ApJ, 689, 1089
- Vink, J., Bleeker, J., van der Heyden, K., Bykov, A., Bamba, A., & Yamazaki, R. 2006, ApJ, 648, 33
- Vink, J., Yamazaki, R., Helder, E.A. & Schure, K.M. 2010, ApJ, 722, 1727
- Vladimirov, A.E., Bykov, A.M., & Ellison, D.C. 2008, ApJ, 688, 1084
- Wagner, A.Y., Lee, J.-J., Raymond, J.C., Hartquist, T.W., & Falle, S.A.E.G. 2009, ApJ, 690, 1412
- Warren, J.S., et al. 2005, ApJ, 634, 376
- Winske, D., Wu, C.S., Li, Y.Y., Mou, Z.Z. & Guo, S.Y. 1985, JGR, 90, 2713
- Zirakashvili, V.N. & Ptuskin, V.S. 2008, in AIP Conference Series, Vol. 1085, (American Institute of Physics), p. 336

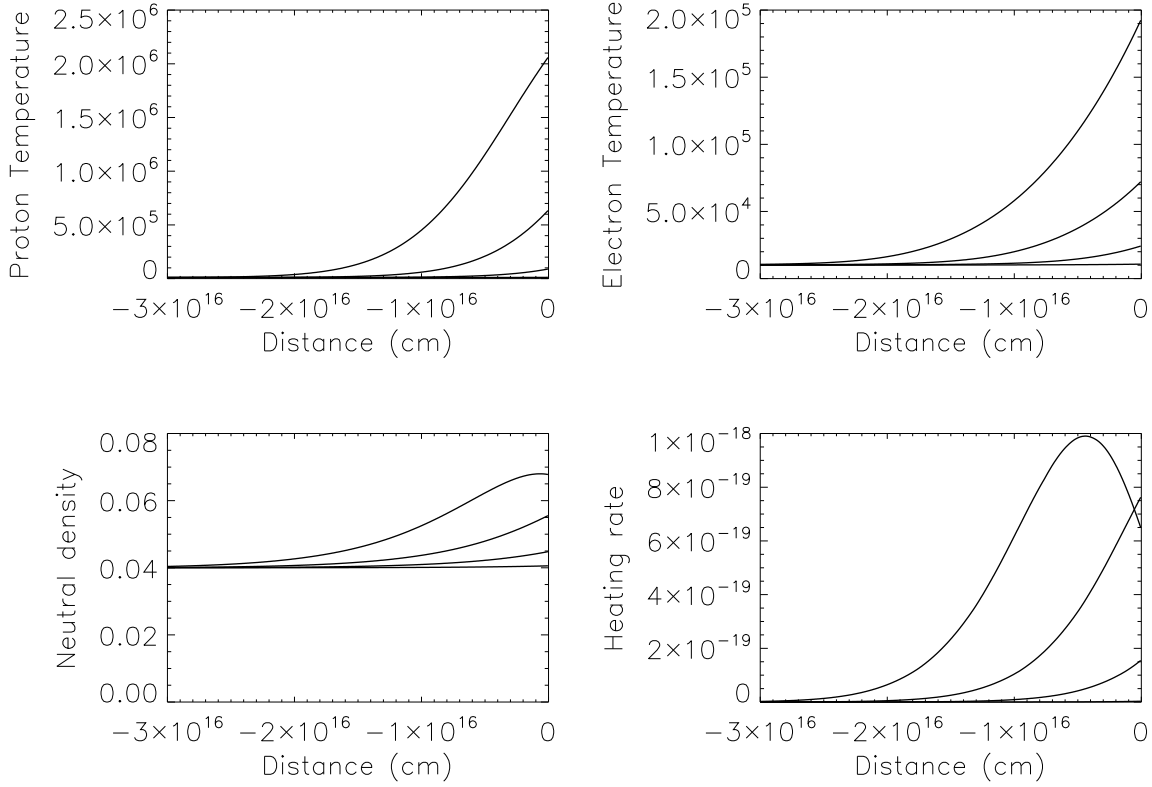


Fig. 1.— Plots of a) proton temperature, b) electron temperature, c) neutral density and d) heating rate for models having $\kappa = 2.0 \times 10^{24} \text{ cm}^2 \text{ s}^{-1}$, pre-shock density = 0.2 cm^{-3} and neutral fraction 0.2. The models assume a post-shock cosmic-ray pressure of 10%, 30%, 50% and 70% of the total pressure, with the 10% curves at the bottom and the 70% curves at the top in all four plots.

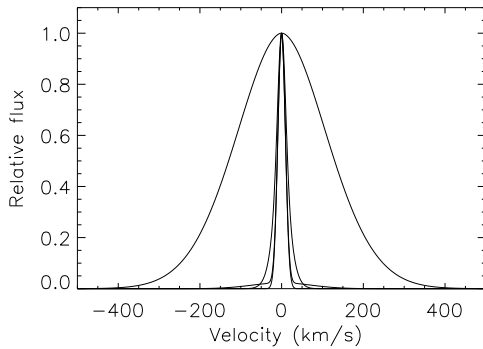


Fig. 2.— Velocity distributions perpendicular to the flow direction at the gasdynamic subshock for the four models shown in Figure 1. Note the narrow central component and broader wings in the model with 50% cosmic-ray pressure and the large width predicted by the 70% cosmic-ray pressure model.

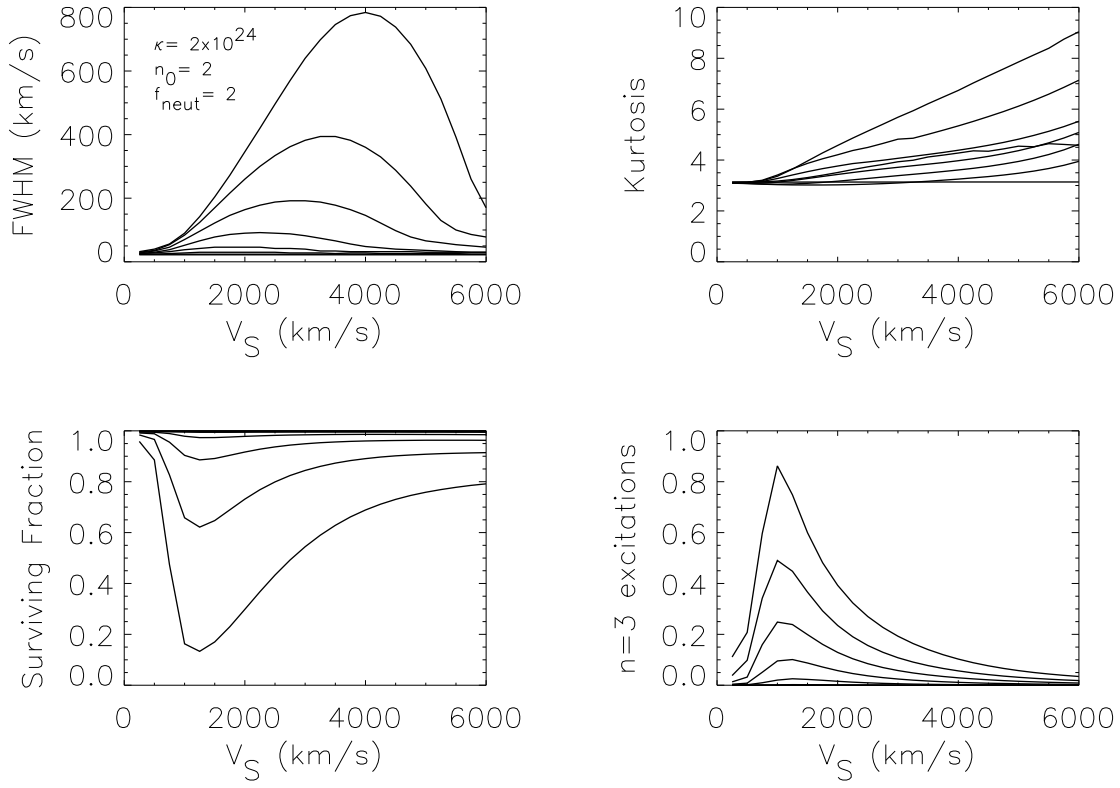


Fig. 3.— Model grid for $\kappa = 2.0 \times 10^{24}$, a pre-shock density of 0.2 cm^{-3} and neutral fraction of 0.2. Models are shown for $P_{CR}/(P_{CR} + P_G) = 0.1$ to 0.8 at the shock front. The panels show the FWHM and kurtosis of neutrals that reach the subshock, the fraction of neutrals that reach the subshock and the number of excitations to $n=3$ in the precursor per incident neutral hydrogen atom. As in Figure 1, the 80% models are the extreme cases.